Int J Clin Exp Med 2015;8(6):8758-8766
www.ijcem.com /ISSN:1940-5901/IJCEM0008797

Original Article

Lung cancer cellular apoptosis induced by recombinant human endostatin gold nanoshell-mediated near-infrared thermal therapy

Haiqing Luo[1,2*], Meng Xu[1*], Xinhai Zhu[1], Jianfu Zhao[1], Shiqing Man[3], Haoran Zhang[3]

[1]Department of Oncology, The First Affiliated Hospital, Jinan University, Guangzhou, 510630, China; [2]Oncology Center, The Affiliated Hospital of Guangdong Medical College, Zhanjiang, 524001, China; [3]Department of Electronic Engineering, Institute of Nano-Chemistry, Jinan University, Guangzhou 510632, China. [*]Equal contributors.

Received April 5, 2015; Accepted June 5, 2015; Epub June 15, 2015; Published June 30, 2015

Abstract: Aims and background: Endostatin can inhibit tumor endothelial cell proliferation, angiogenesis, and growth. We aimed to determine the increase in antitumor capabilities of recombinant human endostatin (rhES) when used with a nanocarrier system. The effect of gold nanoshell particles of recombinant human endostatin (G-rhES) with near-infrared (NIR) irradiation on proliferation, inhibition, and apoptosis of A549 lung cancer cells was studied. Materials and methods: Gold nanoshell particles were prepared. Endostatin was connected with the bond A-U through surface modification by bioconjugation of core-shell structured gold nanoshells. The drug targeting endostatin and the synthesized G-rhES were successfully connected. G-rhES inhibited proliferation of A549 lung cancer cells, as detected using tetrazolium colorimetric assay. Cellular apoptosis was measured by flow cytometry. Mitochondrial membrane potential was determined using a confocal microscope. Morphological changes were studied by atomic force microscopy. Results: Under irradiation in the 820 nm NIR, G-rhES significantly inhibited the proliferation of A549 lung cancer cells. The underlying mechanism may be related to heat-induced apoptosis and cytotoxicity by NIR absorption, which kills cells directly, thereby indicating that G-rhES have good biocompatibility and pharmacological potency. Characterization of the local structure of lung cancer cells showed that G-rhES targeted surface receptors that may serve an apoptotic function under NIR exposure. NIR gold nanoshell particles showed synergism with endostatin, which may be related to hyperthermia-increased cytotoxicity and the apoptotic effect of endostatin. Conclusion: These data suggest that G-rhES can enhance the inhibition of tumor growth. The new treatment strategy of G-rhES combined with thermal therapy may lead to lung cancer remission. The potential benefits of G-rhES are being considered for clinical evaluation.

Keywords: Gold nanoshells, lung cancer, recombinant human endostatin

Introduction

Lung cancer is the most common cause of cancer-related mortality. More than 50% non-small cell lung cancer (NSCLC) patients are diagnosed at an advanced stage of nodal involvement or metastasis. The 5-year survival rate for stage IIIB/IV NSCLC is poor. Standard chemotherapy on NSCLC patients has yielded unsatisfactory antitumor activity. Angiogenesis is involved in lung cancer formation and distant metastases. Anti-angiogenesis is an important strategy against lung cancer [1, 2]. Recombinant human endostatin (rhES) is an endostatin that is expressed and purified from Escherichia coli with an additional nine-amino acid sequence, thereby forming another His-tag structure. rhES suppresses the proliferation, migration, and tube formation of tumor endothelial cells stimulated by vascular endothelial growth factor (VEGF) [3]. rhES blocks the microvessel that sprouts from aortic rings during tumor angiogenesis. rhES also inhibits the formation of new capillaries from pre-existing vessels, there by affecting the growth of vessels in lung cancer [4]. The rhES combined rhES with chemotherapy regimens could improve the median survival time and overall survival rate of patients with advanced lung cancer [5, 6]. However, the plasma concentration of rhES was not stable

because of its short half-life of 10.7 h and rapid clearance from systemic circulation. Therefore, using a new drug delivery carrier with well-controlled release may improve the tumor-killing activity of rhES.

Tumor-targeted therapy based on nanomaterials and nanotechnology can be very useful in lung cancer treatment [7-9]. Nanoparticles are ultramicroscopic and are easily ingested by cancer cells, thereby enhancing anti-tumor effect of chemotherapy. Moreover, nanoparticles can be ideal vectors for drug intracellular transporters [10-12]. Nanoshells can convert light into thermal energy. To assess the anti-tumor activity of gold nanoshell particles of recombinant human endostatin (G-rhES) with near-infrared (NIR) thermal therapy in vitro, we prepared bio-soluble loaded immunological nanoparticles by attaching rhES to a bioconjugation of Au/SiO_2 nanoshells, there by combining G-rhES and NIR light. We observed the synthesis procedures and the slow-release characteristics of G-rhES. We investigated the proliferation and apoptosis of G-rhES-mediated NIR thermal therapy on lung cancer cells in vitro. We presented the experimental results of the combination of G-rhES with NIR thermal therapy. We determined the occurrence of apoptosis in lung cancer cells induced by G-rhES-mediated NIR thermal therapy.

Methods

Reagents and chemicals

Endostatin was purchased from Medgenn Bioengineering Co., Ltd. (Yantai, China). RPMI 1640 medium and fetal bovine serums were purchased from Gibco Inc. (Grand Island, NY, USA). Aminopropyltriethoxysilane (APTES) was purchased from Avocado Research Chemical, Ltd. (NY, USA). Rhodamine 123, tetrazolium (MTT), and analytical grade chemicals were purchased from Sigma Chemical Co. (St. Louis, MO, USA).

Synthesis procedures of recombinant human endostatin gold nanoshells

About 120 nm amorphous submicrometer spheres of silica were synthesized by base-catalyzed hydrolysis of tetraethoxysilane (TEOS) via Stöber process. The surface of silica particles were terminated with amine groups by reaction with APTES. Small-sized gold colloids (1 nm to 2 nm) were synthesized according to Stuff [13]. The aminated silica particles were added to the fine gold colloid suspension to attach the gold colloid to the dielectric nanoparticle surfaces via molecular linkages. Silica nanoparticle covered with islands of gold colloid (which served as "seed") were used. The final nanoshells would develop based on these islands of gold colloid, eventually coalescing with neighboring colloids to form a complete gold shell. For bioconjugation of the Au/SiO_2 nanoshells, the common protein linker of 2-iminothiolane was used. This linker could react with the amidogen of protein and release the SH group. Thiol chemistry has been widely used for the modification of gold surfaces [14, 15], and the released thiol was used for the same purpose. The 2-iminothiolane was dissolved in the K_2CO_3 solution (pH 8.5) and subsequently mixed with a proper amount of Au nanoshells and rhES. Thus, the molar ratio of rhES to 2-iminothiolane was 1:1. The sample was allowed to react overnight, after which it was washed by repeated cycles of centrifugation and redispersion (six times) in water. Samples were dried in vacuum at 30°C to obtain the final samples.

G-rhES-mediated NIR thermal therapy in vitro

Human lung cancer cell line A549 was provided by the Institute of Cell Biology, Chinese Academy of Medical Science. Cells were cultured in RPMI-1640 supplemented with 10% heat-inactivated fetal calf serum, 4 mM glutamine, 100 U/ml penicillin, 1 μg/ml glucose, and 0.25 U/ml insulin under 37°C, 5% CO_2, 95% air, and 95% humidity. A549 lung cancer cells were exponentially grown on log phase and treated as follows: (1) in the control group, cells were incubated in a saline medium for 12 h to 48 h; (2) in the G-rhES-mediated NIR thermal therapy, cells were treated with G-rhES and exposed to NIR light (820 nm, 35 w/cm^2) from NIR laser machine (EO-CT80E, China) for 7 min to induce cellular toxicity by thermal therapy. After NIR light treatment, cells were incubated for 2 h at 37°C.

MTT colorimetric assay

The cytotoxic effects of G-rhES with NIR thermal therapy were determined by MTT colorimetric assay. A549 lung cancer cells (2×10^4 cells/well) were seeded into a 96-well plate and allowed to attach overnight. Subsequently, 10 μl of 5 mg/ml MTT solution was added to each well. The plates containing cells were incubated

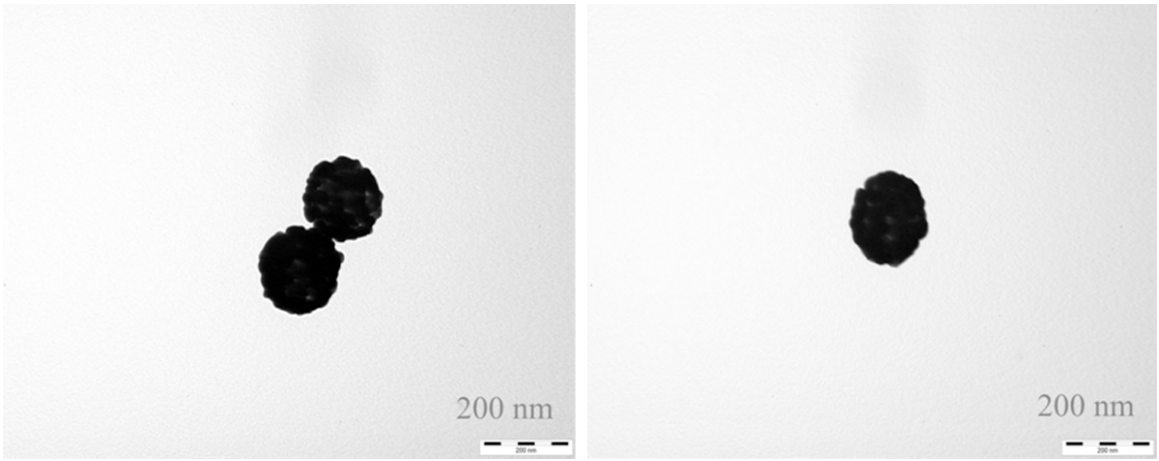

Figure 1. The core-shell structure of SiO_2/Au nanoparticles. Transmission electron microscopy showed that nanoparticles SiO_2/Au nanoparticles were round particles with relatively smooth edges. Micro-gold nanocolloids were well distributed and adsorbed on the surface of SiO_2.

for another 4 h at 37°C. The media was then aspirated. The blue formazan crystals were completely dissolved after the addition of 100 μl DMSO. The absorbance at a wavelength of 570 nm was measured with a multi-well spectrophotometer (BioTek, VT, USA). Cell growth inhibitory rate was calculated as a percentage of the treated groups to the untreated controls (no thermal therapy).

Apoptotic cell death assay

The apoptosis of A549 lung cancer cells induced by G-rhES and NIR thermal therapy was determined by Flow cytometry (**Appendix Figure 1**). Cells samples were fixed with 4% paraformaldehyde solution for 30 min at room temperature. Cells were harvested by centrifugation, and the cell pellets were resuspended in lysis buffer (0.1% sodium citrate and 0.1% Trixon-100) containing 50 μg/ml of propidium iodide. Samples were stored at 4°C for 1 h before FACScan detection and analysis of sub-G_1 DNA content.

Detection of mitochondrial membrane potential (MMP) by confocal microscope

MMP was determined through a confocal microscope. Cells were washed in PBS buffer after drug treatment. Cells were incubated for 15 min with fluorescence probe 5 μg/ml Rhodamine 123 for MMP at 37°C in a 5% CO_2 humidified incubator. In all cases, samples were mounted on glass slides for observation under a confocal microscope (ACASS570, Meridian, USA).

Atomic force microscope detection

A549 lung cancer cells were vaccinated on the slide with lysine, fixed with 2.5% glutaricdialdehyde for 10 min, flushed with deionized water. Subsequently, cells were air dried. The scanned region of the samples of the cells for image formation was fixed on the glass by using atomic force microscopy. The experiment required 100 μm scanners and a UL20B silicon probe with a force constant of 2.8 N/m. Scanning was conducted, and each group of samples contained more than 10 cells. The images were observed using an autoprobe CP atomic force microscope (Veeco, USA). The software that came with the instrument (Thermo Microscopes Proscan Image Processing Software Version 2.1) was used to collect and process the image data.

Statistical analysis

Results were reported as mean ± standard error of the mean. The statistical significance between two measurements was determined by the two-tailed unpaired Student's *t*-test. Probability values of $P < 0.05$ were considered significant.

Results

Characteristics of G-rhES

Synthesis and bioconjugation of core-shell structured gold nanoshells were performed to prepare silicon oxide nanoshell particles, which were coated on the surface for effective and

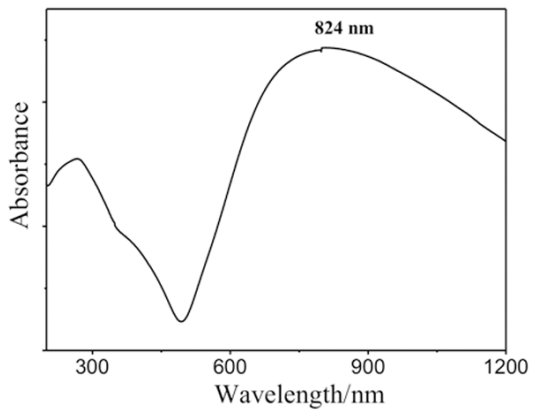

Figure 2. Optical absorption spectrum of SiO_2/Au nanoparticles. The wavelength (824 nm) produced optimal nanoshells heating.

complete payment shells. The surface modification was required to connect rhES. 2-Iminothiolane was used to close the shells and nonspecific sites of the surface layer to increase biocompatibility of G-rhES. The method of preparation was satisfactory, simple, and reproducible. Transmission electron microscopy was employed to study the shape of the G-rhES. The prepared G-rhES was small, sturdy, and easily absorbed. The average diameter of G-rhES was 120 nm (**Figure 1**), and the drug envelope ratio was 37.5%. Gold shells resulted in a peak absorbance at 824 nm, which was identical to the emission wavelength of NIR laser (**Figure 2**).

Inhibition of lung cancer cells induced by G-rhES and NIR thermal therapy

The significant inhibition of proliferation of A549 lung cancer cells by G-rhES and *NIR thermal therapy* was observed. G-rhES inhibited proliferation at 820 nm in treated A549 lung cancer cells compared with normal A549 lung cancer cells. G-rhES combined with NIR irradiation showed growth inhibition of A549 lung cancer cells in a dose-and time-dependent manner. G-rhES and NIR evidently inhibited A549 cells (**Figure 3**; **Table 1**).

Flow cytometry (**Appendix Figure 1**) results indicated that 10 μg/ml to 40 μg/ml dosages of G-rhES at 820 nm could induce apoptosis of A549 lung cancer cells. The apoptosis of graphics showed that G-rhES combined with hyperthermia could increase apoptosis of A549 lung cancer cells. Moreover G-rhES not only promoted apoptosis of A549 lung cancer cells, but also directly killed the cells in a dose-dependent manner (**Table 2**).

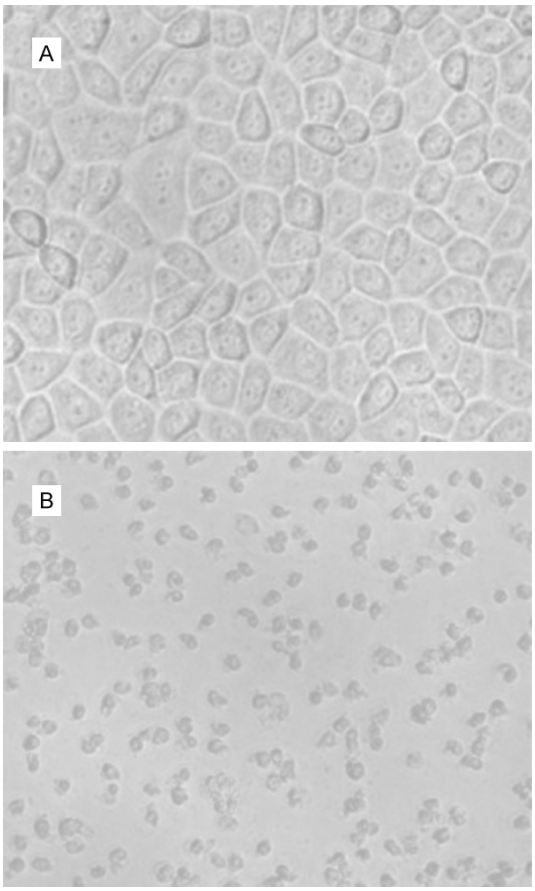

Figure 3. The morphological manifestation of lung cancer cells treated with G-rhES nanoshells and NIR. A: normal A549 cells (×40); typical morphological images of cells were observed. B: A549 cells treated with G-rhES and NIR; the apoptotic cells shrank markedly (×40).

Effect of G-rhES and NIR on MMP

Measurement of MMP by the fluorescent probe Rhodamine 123 showed that the fluorescent intensity (FI) of MMP was 1752.1±278.7 U in the control group. The FI value was increased to 3050.8±118.2 U ($P < 0.05$) in the G-rhES and NIR-treated group (**Figures 4**, **5**). An increase in mitochondrial fluorescence of Rhodamine 123 represented the addition in mitochondrial potential depolarization, thereby indicating the reduction of MMP level. Furthermore, the decrease of MMP level occurred with apoptotic cellular damage induced by G-rhES and NIR irradiation.

Table 1. Inhibition rate of NIR irradiation and different concentrations of G-rhES, as tested by MTT chromatometry

Concentration (μg/ml)	24 h		48 h		72 h	
	A value	Inhibition rate (%)	A value	Inhibition rate (%)	A value	Inhibition rate (%)
0	1.438±0.02	-	1.521±0.02	-	1.530±0.01	-
2.5	1.419±0.04	1.2	1.484±0.02	2.4	1.477±0.01	3.4
5	1.380±0.01	4.0	1.431±0.01	5.9	1.433±0.03	6.3
10	1.374±0.01	4.4	1.425±0.04	6.3	1.373±0.04	10.2
20	1.240±0.03	13.7	1.280±0.05	15.8	1.570±0.02	17.8
40	1.196±0.04	16.8	1.239±0.03	18.5	1.138±0.01	25.1
80	1.139±0.05	20.7	1.131±0.01	25.6	1.069±0.04	30.1

P<0.05 compared with the control group.

Table 2. Apoptosis rates of A549 lung cancer cells with G-rhES combined with NIR irradiationco-cultured for 72 h

Concentration (μg/ml)	Apoptotic rate (%)
0	0.9±0.1
10	5.4±2.3*
20	15.9±4.9*
40	21.4±2.8*

*p<0.01 compared with the group of negative control-nanoshells.

Morphological changes of lung cancer cells induced by G-rhES and NIR

The inhibitory effects of G-rhES and NIR irradiation on lung cancer cells were detected at the nanometer scale. The morphological differences of the overall shape and surface membrane were studied by high-resolution atomic force microscopy imaging. Morphological parameters of the valley-to-peak and average surface roughness of cells were studied. Atomic force microscopy results showed significant micromorphological changes in the A549 lung cancer cells treated with G-rhES under irradiation in the 820 nm NIR spectrum. The overall framework of cells still existed, but the number of pseudopodia decreased compared with the control group. Many small holes appeared on the surface of the cellular membrane. The holes of the cell surface were irregular, and cytoplasm flowed out. These morphological changes indicated apoptotic cellular morphological damage induced by G-rhES and NIR irradiation.

Discussion

Initiation of angiogenesis results in tumor growth, metastases, and progression. Endostatin is a new spectrum angiogenesis inhibitor that could be a molecular target agent for co-administration with other therapies during lung cancer treatment. Nanotechnology research in the field of tumor treatment has generated tremendous developments. For example, multidrug resistance (MDR) in lung cancer is the primary reason for chemotherapy failure. Reversing MDR specific inhibitors might increase chemosensitization [16-18], but anti-EGFR antibody conjugated gold nanoparticles with laser photothermal therapy were used to treat epithelial carcinoma [19, 20]. The efficacy of angiogenesis inhibitor still requires improvement. Ideal properties of angiogenesis inhibitors include broad spectrum of activity, lack of drug resistance, relative nontoxicity, and synergistic activity with other anticancer drugs, such as bevacizumab, which is a recombinant humanized monoclonal anti-VEGF antibody that recognizes and neutralizes isoforms of VEGF.

Angiogenesis target therapy plays an important role in lung cancer. Tumor cells can only survive if they are able to obtain the steady supply of oxygen and other nutrients, which these cells need to support their metabolic activity. Endostatin can improve the efficacy of chemotherapy in lung cancer [5]. The main steps of the angiogenic process can be interrupted by inhibiting endogenous angiogenic factors, such as bFGF and VEGF, suppressing degradative enzymes responsible for the degradation of the basement membrane of blood vessels and for decreasing endothelial cell proliferation and migration. Endostatin showed synergistic activity when used in combination with chemotherapeutic agents (vinorelbine and cisplatin) and showed favorable toxicity in advanced lung cancer patients. Endostatin with systemic che-

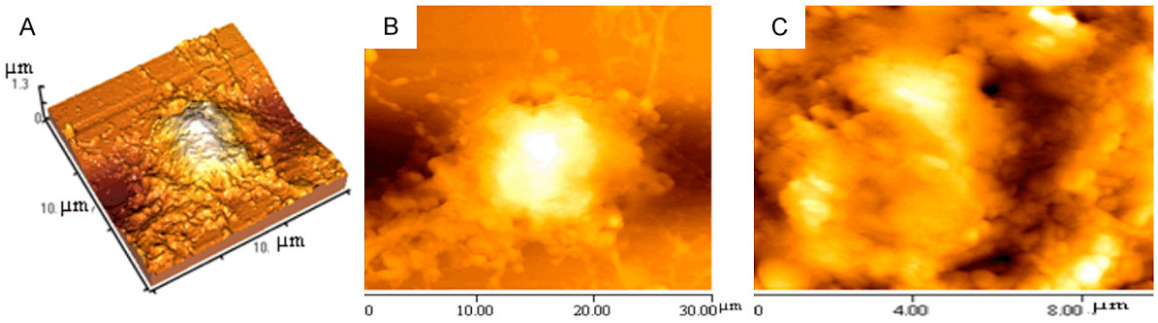

Figure 4. Morphological changes in A549 lung cancer cells treated with 40 μg/ml G-rhES and NIR irradiation by atomic force microscopy. A: Cell-surface 3D map in the error signal image. B: Cell average length was 27.4 μm; the average width was 15.5 μm; the morphological parameter of peak to valley (Rp-v) was 1279±115 nm; and the surface roughness ($_{Ra}$) was 2542±187 nm. C: Corresponding ultrastructure of the membrane of G-rhES-treated cells from an area in the left image.

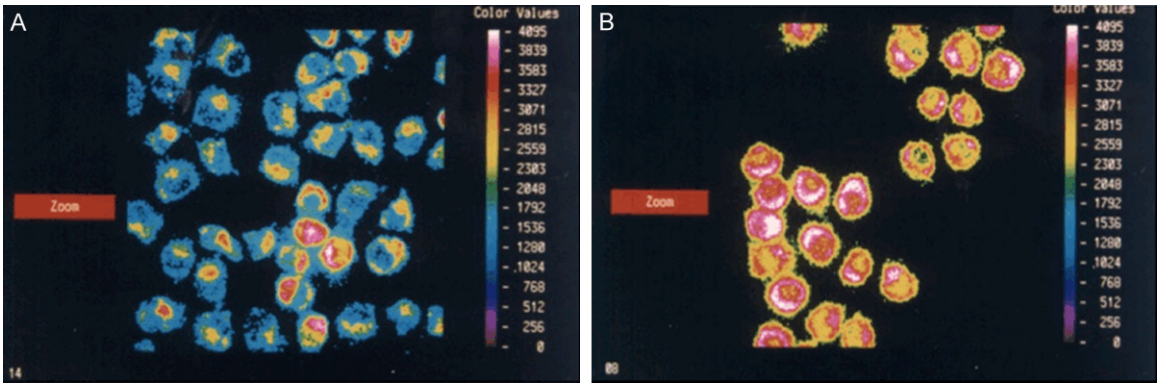

Figure 5. Digital images of MMP fluorescence induced by G-rhES and NIR irradiation. A was in the control group. B was in the G-rhES nanoshells and NIR irradiation group.

motherapy enhanced antitumor efficacy in liver metastasis of colorectal cancer.

We studied the occurrence of lung cancer cells apoptosis induced by G-rhES-mediated NIR thermal therapy. Results showed that the synthesis and bioconjugation of G-rhES along with NIR had significant efficiency and were superior to those without G-rhES and NIR. Colloidal gold nanospheres are promising as therapeutic agents because of their simple and fast preparation [21]. G-rhES and NIR significantly inhibited proliferation of lung cancer cells. G-rhES could promote apoptosis of lung cancer cells. The evident apoptotic morphological changes, which include changes in the overall shape and surface membrane of cells, were studied by atomic force microscopy imaging. High-resolution atomic force microscope imaging can be used to evaluate therapeutic effect on morphological parameters in detail [22-24]. Mitochondria play an important role in induction of apoptotic cell death. A collapse in inner transmembrane potential indicated the opening of a large conductance channel, known as the mitochondrial permeability transition pore, which releases caspases-activating proteins located within the inter membrane space into the cytosol. Data showed a fall of MMP level that occurred during apoptotic cellular damage. Data on apoptotic cellular morphological changes induced by recombinant human endostatin gold nanoshell and NIR were also presented.

The effect of G-rhES and NIR on lung cancer in vivo will be investigated in the future. The signal transduction of G-rhES and methods to inhibit angiogenesis of lung cancer will be investigated. The new treatment strategy of G-rhES combined with hyperthermia may help with lung cancer remission.

Acknowledgements

The study was supported by the National Natural Science Foundation of China (8127-3814) , Science and Technology Foundation of Guangzhou (2007Z3-D2051).

Disclosure of conflict of interest

None.

Abbreviations

rhES, Recombinant human endostatin; G-rhES, Gold nanoshell particles of recombinant human endostatin; NIR, Near-infrared; APTES, Aminopropyltriethoxysilane; NSCLC, Non-small cell lung cancer; VEGF, Vascular endothelial growth factor; MTT, Rhodamine 123, tetrazolium; MMP, Mitochondrial membrane potential; FI, Fluorescent intensity; MDR, Multidrug resistance.

Address correspondence to: Meng Xu, Department of Oncology, The First Affiliated Hospital, Jinan University, Guangzhou, 510630, China. Tel: +8620-3868-8908; Fax: +8620-3868-0000; E-mail: xumengjinan@yahoo.com

References

[1] Scappaticci FA. Mechanisms and future directions for angiogenesis-based cancer therapies. J Clin Oncol 2002; 20: 3906-3927.

[2] Schettino C, Bareschino MA, Rossi A, Maione P, Sacco PC, Colantuoni G, Rossi E, Gridelli C. Targeting angiogenesis for treatment of NSCLC brain metastases. Curr Cancer Drug Targets 2012; 12: 289-299.

[3] Folkman J. Anti-angiogenesis in cancer therapy-endostatin and its mechanisms of action. Expt Cell Res 2006; 312: 594-607.

[4] Eichholz A, Merchant S, Gaya AM. Anti-angiogenesis therapies: their potential in cancer management. Onco Targets Ther 2010; 3: 69-82.

[5] Dienstmann R, Martinez P, Felip E. Personalizing therapy with targeted agents in non-small cell lung cancer. Oncotarget 2011; 2: 165-177.

[6] Nagy K, Székely-Szüts K, Izeradjene K, Douglas L, Tillman M, Barti-Juhász H, Dominici M, Spano C, Luca Cervo G, Conte P, Houghton JA, Mihalik R, Kopper L, Peták I. Proteasome inhibitors sensitize colon carcinoma cells to TRAIL-induced apoptosis via enhanced release of Smac/DIABLO from the mitochondria. Path Onco Res 2006; 12: 133-142.

[7] Fletcher JI, Haber M, Henderson MJ, Norris MD. ABC transporters in cancer: more than just drug efflux pumps. Nat Rev Cancer 2010; 10: 147-156.

[8] Loo C, Lowery A, Halas N, West J, Drezek R. Immunotargetednanoshells for integrated cancer imaging and therapy. Nano Lett 2005; 5: 709-711.

[9] Marcato PD, Favaro WJ, Duran N. Cisplatin Properties in a Nanobiotechnological Approach to Cancer: A Mini-Review. Curr Cancer Drug Targets 2014; [Epub ahead of print].

[10] Kam NW, O'Connell M, Wisdom JA, Dai H. Carbon nanotubes as multifunctional biological transporters and near-infrared agents for selective cancer cell destruction. PNAS 2005; 102: 11600-11605.

[11] Hirsch LR, Stafford RJ, Bankson JA, Sershen SR, Rivera B, Price RE, Hazle JD, Halas NJ, West JL. Nanoshell-mediated near-infrared thermal therapy of tumors under magnetic resonance guidance. PNAS 2003; 100: 13549-13554.

[12] Salerno M, Cenni E, Fotia C, Avnet S, Granchi D, Castelli F, Micieli D, Pignatello R, Capulli M, Rucci N,Angelucci A, Del Fattore A, Teti A, Zini N Giunti A, Baldini N. Bone-targeted doxorubicin-loaded nanoparticles as a tool for the treatment of skeletal metastases. Curr Cancer Drug Targets 2010; 10: 649-659.

[13] Stöber W, Fink A, Bohn E. Ordered mesoporous silica in the micron size range. Colloid Interface Sci 1968; 26: 62-69.

[14] Wang M, Thonou M. Targeting nanoparticles to cancer. Pharmacol Res 2010; 62: 90-99.

[15] Zhang HR, Man SQ, Xu M, Zhu XH. Control Synthesis and Bioconjugation of Core-Shell Structured Gold Nanoparticles. Chin J Inorganic Chemistry 2010; 26: 1768-1775.

[16] Xu M, Hu SSC, Zhang JR. Analysis of Multidrug Resistance-Associated Protein (MRP) Gene and Chemosensitivity Testing in Non Small Cell Lung Cancer (NSCLC) Patients. J Tumor Marker Onco 2000; 15: 235-244.

[17] Xu M, Sheng L, Zhu X, Zeng S, Chi D, Zhang GJ. Protective effect of tetrandrine on doxorubicin-induced cardiotoxicity in rats. Tumori 2010; 96: 460-464.

[18] Xu M, Sheng LH, Zhu XH, Zeng SB, Zhang GJ. Reversal effect of Stephaniatetrandra-containing Chinese herb formula SENL on multidrug resistance in lung cancer cell line SW1573/2R120. Am J Chin Med 2010; 38: 401-413.

[19] Mainardes RM, Silva LP. Drug delivery systems: past, present, and future. Curr Drug Targets 2004; 5: 449-455.

[20] El-Sayed IH, Huang X, El-Sayed MA. Selective laser photo-thermal therapy of epithelial carci-

noma using anti-EGFR antibody conjugated gold nanoparticles. Cancer Lett 2006; 239: 129-135.
[21] Huang X, Jain PK, El-Sayed IH, El-Sayed MA. Gold nanoparticles: interesting optical properties and recent applications in cancer diagnostics and therapy. Nanomed 2007; 2: 681-693.
[22] Lee JH, Huh YM, Jun YW, Seo JW, Jang JT, Song HT, Kim S, Cho EJ, Yoon HG, Suh JS, Cheon J. Artificially engineered magnetic nanoparticles for ultra-sensitive molecular imaging. Nat Med 2007; 13: 95-99.
[23] Xu RX, Povoski SP. Diffuse optical imaging and spectroscopy for cancer. Expert Rev Med Devices 2007; 4: 83-95.
[24] Goksu EI, Vanegas JM, Blanchette CD, Lin WC, Longo ML. AFM for structure and dynamics of biomembranes. Biochim Biophys Acta 2009; 1788: 254-266.

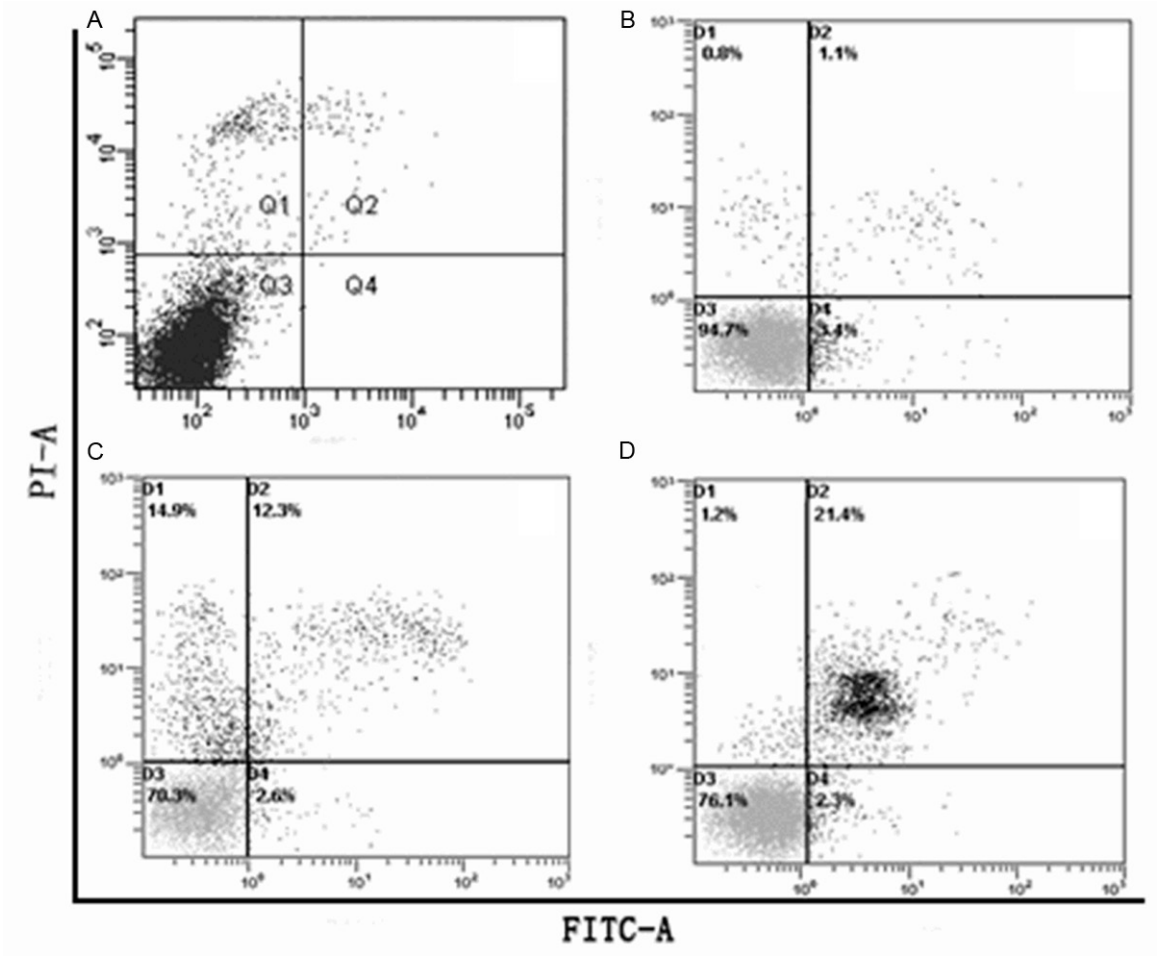

Appendix Figure 1. A549 lung cancer cells treated with 10 μg/ml to 40 μg/ml dosages of G-rhES and NIR irradiation were double-stained with PI and Annexin V, and then analyzed by flow cytometry. A: The control group. B: 10 μg/ml G-rhES and NIR irradiation group. C: 20 μg/ml G-rhES and NIR irradiation group. D: 40 μg/ml G-rhES and NIR irradiation group.